

Effect of Diethylene Glycol (DEG) on the Crystallization Behavior of Poly(ethylene terephthalate) (PET)

MAHESH PATKAR and S. A. JABARIN*

Polymer Institute, College of Engineering, The University of Toledo, Toledo, Ohio 43606-3390

SYNOPSIS

The effect of diethylene glycol (DEG) on the crystallization of poly(ethylene terephthalate) (PET) was studied under isothermal and dynamic conditions. The strain-induced crystallization of PET and its relationship to DEG content was also studied. The samples were isothermally and dynamically crystallized in the differential scanning calorimeter (DSC). The thermograms were then analyzed to determine the kinetic parameters. Strain-induced crystallization was studied by stretching samples at different strain rates. These samples were then annealed for various periods of time and quenched to room temperature. Birefringence and density were measured on the annealed samples. Results indicate that the DEG content reduces the rate of crystallization of PET when crystallizing from the melt, isothermally and dynamically. When crystallizing from the glassy state, the effects of DEG are not prominent. The mechanism of crystallization is not affected by the amount of DEG, within the range of DEG contents evaluated. In the case of strain-induced crystallization, increased DEG content reduces the crystallinity of PET at intermediate strain rates, but at higher strain rates, the crystallinity is not affected by the DEG content. © 1993 John Wiley & Sons, Inc.

INTRODUCTION

Diethylene glycol (DEG) is formed in a side reaction under the conditions of industrial synthesis of PET from dimethyl terephthalate and ethylene glycol. Hence, commercial PET almost always presents a random copolymer containing diethylene glycol terephthalate (DEGT). The diethylene glycol content in commercial PET is around 2–4 mol %. Its presence affects many important properties of PET such as crystallization behavior, thermal stability, dyeability, etc.¹

Frank and Zachmann² investigated samples with DEG contents up to 15 mol %. Their study shows that when crystallizing from the melt, increasing the DEG content increases the half-time of crystallization, indicating a decrease in the rate of crystallization. When crystallizing from the glassy state, rate of crystallization increases with increasing DEG content. They explained these differences as being

associated with the decrease of T_m and T_g with increasing DEG contents.

Farikov et al.³ confirmed the decrease in T_m and T_g with increase in the DEG concentration. They concluded that when crystallizing from the glassy state, at crystallization temperatures higher than 200°C, the crystallization rate decreases with increasing DEG content; but at lower temperatures, it is insensitive to the DEG content.

Golike and Cobbs⁴ studied the crystallization of PET, when cooling from the melt, for samples containing 5 and 10 mol % DEG at crystallization temperatures ranging from 110 to 240°C. They concluded that at temperatures just above T_g , where molecular motion is rate-determining, higher DEG content increases the rate of crystallization. This was attributed to the flexible aliphatic chains introduced by the presence of DEG. At higher temperatures, where the rate is determined by the degree of supercooling, addition of the copolymer decreases the crystallization rate.

Yu et al.¹ used differential scanning calorimetry (DSC), small angle light scattering (SALS), and polarized light microscopy (PLM) to study the

* To whom correspondence should be addressed.

crystallization behavior of PET and its relation to DEG content. The results showed that the rate of crystallization decreases with increased DEG content, when crystallizing from the melt. The effect is not so prominent when crystallizing from the glassy state.

Farikov⁵ used small-angle X-ray scattering to study PET samples with different DEG contents (up to 15 mol %). It was found that the equilibrium crystallinity decreases with increased DEG content. This was attributed to the larger intralamellar amorphous regions with lower density than that of the crystalline regions.

Most workers conclude that increased concentrations of DEG cause the rate of crystallization to decrease when crystallizing isothermally from the melt. When crystallizing from the glassy state, however, some workers conclude that the rate of crystallization of PET increases with increasing DEG content. Others find that DEG does not affect the isothermal crystallization of PET from the glassy state. The effect of DEG on the dynamic crystallization of PET has not been studied.

Recently, Jabarin⁶ studied the strain-induced crystallization of PET. It was found that at low levels of orientation there was no crystallization as measured by birefringence. At intermediate orientation levels, there was an initial decrease in birefringence followed by a gradual increase. At high levels of orientation, the birefringence increases rapidly at first before leveling off.

Since orientation is affected by molecular structure, it is anticipated that DEG will have an effect on the strain-induced crystallization of PET. The present study investigates the crystallinity induced in PET due to orientation and its relationship to DEG content. In addition, the change in crystallization rate and mechanism of crystallization with DEG content is studied. The crystallinity is measured using calorimetry, density, and birefringence.

The following types of crystallization are studied:

- (a) Isothermal crystallization from the melt and the glassy state.
- (b) Dynamic crystallization from the melt.
- (c) Strain-induced crystallization produced by stretching.

EXPERIMENTAL

Materials

Materials, in the form of sheets extruded at 275°C, were provided by Eastman Chemicals. The thickness of the sheets was around 20 mil.

Sample	DEG wt %	I.V. (inherent viscosity)
x20932-190	1.40	0.71
x21467-132	2.08	0.71
x20932-162	2.94	0.69

The mole fraction of DEG is approximately twice the weight fraction. The density of all three samples was 1.3375 g/cm³, which is close to the density of completely amorphous PET. Thus, the crystallinity in the samples was very low.

Thermal Analysis

The crystallization kinetics of PET samples, in the form of sheets, were studied using a Perkin-Elmer DSC-2. The samples were dried overnight at 50°C in a vacuum oven before analyses. The sample weight was around 10 mg. The tests were performed in a nitrogen atmosphere using an empty aluminum pan as reference.

A typical DSC curve obtained for a PET sample with 1.4% DEG when heated at 10°C/min is shown in Figure 1. The step change in the base line around 80°C is the glass transition temperature. This is followed by an exotherm indicating crystallization. When the sample is heated further, an endotherm is observed with a peak temperature around 250°C. Complete melting takes place at 275°C. Therefore, it is concluded that heating the sample to 280°C will sufficiently produce the conditions for complete melting.

Isothermal Crystallization from the Melt

The PET sample was heated to 280°C at a rate of 80°C/min and held for 10 min to ensure complete melting. It was then cooled to the predetermined temperature at a rate of 320°C/min.

Isothermal Crystallization from the Glassy State

The PET sample was heated to 280°C at a rate of 80°C/min and held for 10 min to ensure complete melting. It was then quenched to 40°C at a rate of 320°C/min to obtain a completely amorphous sample. It was then reheated at a rate of 320°C/min to the required temperature.

Dynamic Crystallization

The PET sample was heated to 280°C at a rate of 80°C/min and held for 10 min to ensure complete melting. It was then cooled at different rates to 40°C.

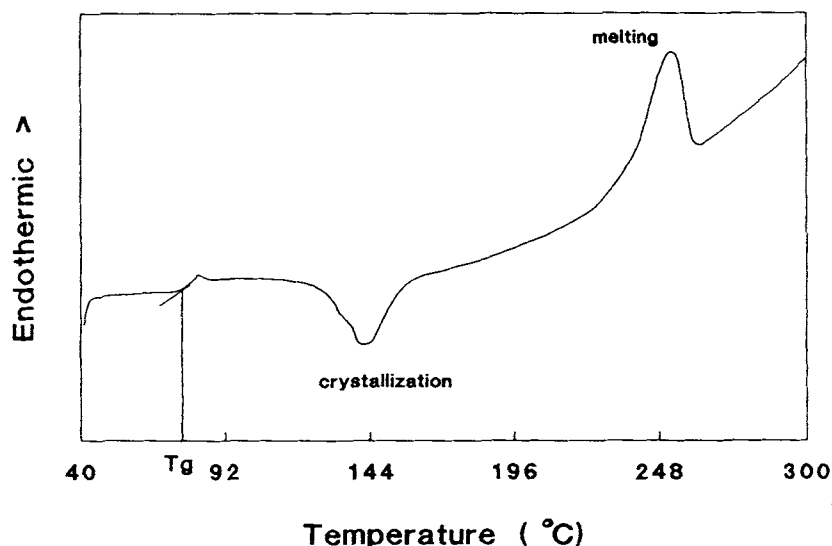


Figure 1 DSC thermogram for PET (1.4% DEG); I.V. = 0.71.

Strain-Induced Crystallization

The long extensional tester (LET) was used to study the strain-induced crystallization. PET sheets were cut into square samples of size 2.375×2.375 in. and stored for 72 h in a 50% relative humidity environment at 23°C prior to testing. This ensures that all the samples are tested under uniform conditions since the moisture content affects the crystallization of PET.

The temperature controls of the LET were set to the stretching temperature of 100°C . After the temperature was reached, the sample was loaded in between the clamps. It was held for 2 min so that there was temperature equilibrium throughout the sample. It was then stretched at different rates (0.25, 0.5, 1 in./s) and annealed for different amounts of time (0–10 min), after which the sample was quickly quenched to room temperature for subsequent measurements. During the stretching and annealing, the stress-strain and the stress-relaxation curves were recorded.

Measurement of Birefringence

The birefringence was calculated from the refractive indices measured in the three principal directions using an Abbe-3L refractometer equipped with a polarizing eyepiece using the procedure developed by Okajima et al.⁷ The temperature was maintained at 25°C .

Measurement of Density

The density of the stretched PET samples was determined at 25°C , in a density gradient column containing calcium nitrate solution.

RESULTS AND DISCUSSION

Equilibrium Melting Temperature: (T_m^0)

In contrast to pure, highly crystalline low molecular weight materials that melt at exactly well-determined temperatures, the fusion of semicrystalline polymers such as PET takes place over a range of temperatures. Such behavior is attributed to crystallite-size distribution. Crystallites with smaller dimensions (thinner) melt at lower temperatures, whereas those with larger dimensions (thicker) melt at higher temperatures.

To determine the equilibrium melting temperature, PET was crystallized from the melt at various temperatures and then heated at the rate of $10^\circ\text{C}/\text{min}$ to determine the melting peak temperature (T_m). The crystallization temperature (T_c) was then plotted against T_m . The theory of polymer crystallization predicts that the characteristic melting temperature should increase linearly with crystallization temperature up to the equilibrium melting temperature⁸ according to the following equation developed by Hoffman and Weeks:

$$T_m = T_m^0(1 - 1/\eta) + T_c/\eta$$

where η is a constant depending on the crystal dimensions.

Hence, extrapolating the plot of T_m vs. T_c to the temperature where T_m is equal to T_c will give T_m^0 as shown in Figure 2.

The values of glass transition temperatures (T_g) and equilibrium melting temperatures (T_m^0) are listed in Table I. The glass transition temperature

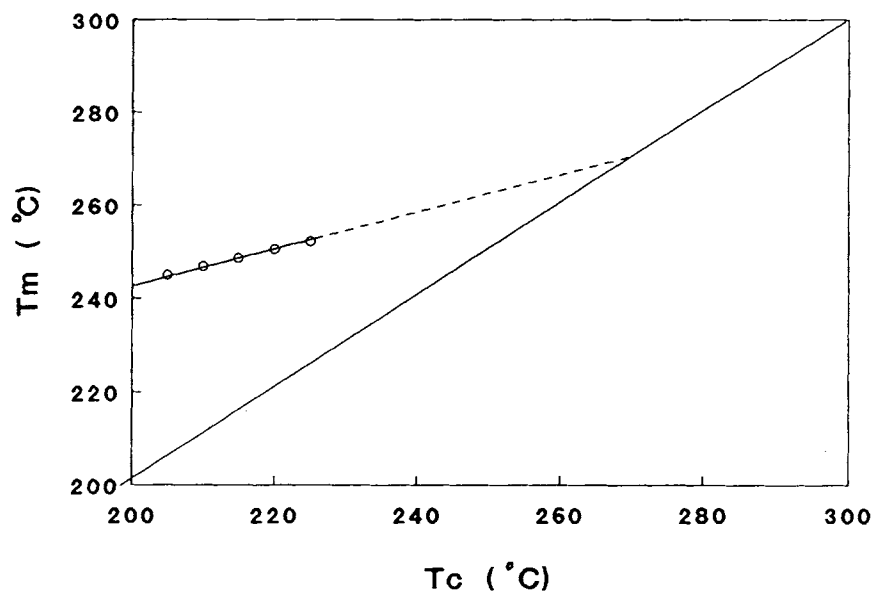


Figure 2 Measurement of equilibrium melting temperature.

is the temperature above which the polymer is flexible and rubbery and below which it is hard, brittle, and glassy. In the glassy state, large-scale molecular motion does not take place. The only molecular motion is that of vibration of atoms. The glass transition corresponds to the onset of liquidlike motion of much longer segments of molecules. T_g decreases with increase in DEG content. The presence of DEG in the main chains of PET increases the ratio of the aliphatic part to the aromatic part. This causes the flexibility of the chains to increase. Hence, the T_g decreases with increasing DEG content.

T_m^0 also decreases with increased DEG content because the presence of DEG introduces imperfections in the PET crystals. This causes the melting-point depression.

Isothermal Crystallization from Melt

The thermograms obtained from the DSC at various temperatures of crystallization are shown in Figure 3. The heat content of the sample is plotted as a function of time. When crystallization begins, an exotherm is observed. The induction time of crystallization is the time required for the crystallization to commence after the crystallization temperature is reached. The induction time can be seen to increase with increase in temperature. This is due to the decrease in the nucleation rate at temperatures near the melting point.

The calorimeter measures the rate of evolution of heat as a function of time. The weight fraction

of the crystallized material X_t at time t is calculated as follows:

$$X_t = \int_0^t (dH/dt) dt / \int_0^\infty (dH/dt) dt$$

where dH/dt is the rate of evolution of heat. Thus, X_t is the ratio of the area under the crystallization endotherm at any time t to the area under the endotherm when the crystallization is complete. The fraction of the uncrystallized material at any time t is

$$\theta_a = 1 - X_t$$

Typical crystallization isotherms at different temperatures are shown in Figure 4 where θ_a is the fraction of uncrystallized material.

The induction times (t_{ind}) and half-times ($t_{0.5}$) of crystallization are listed in Table II. The increase in induction time with DEG content is due to the slower rate of nucleation. The half-time of crystallization is the time required for the material to reach

Table I T_m^0 and T_g for Different PET Samples

DEG (Wt %)	T_g (°C)	T_m (°C)
1.40	77.2	267.7
2.08	76.7	266.0
2.94	74.1	264.2

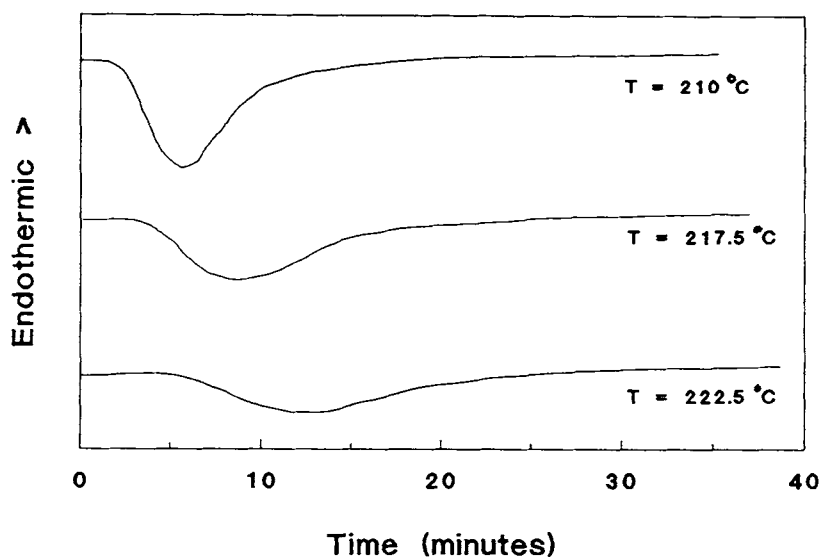


Figure 3 DSC thermograms for isothermal crystallization at various temperatures for PET (1.4% DEG); I.V. = 0.71.

50% of its final crystallinity. The half-time also increases with DEG content because the crystallization is impeded by the presence of DEG.

The crystallization kinetics of polymers is given by Avrami's equation⁹:

$$\theta_a = \exp(-kt^n) \tag{1}$$

where k is the kinetic constant and n is the Avrami exponent describing the mechanism of crystallization.

Here, k is a function of n although this is not explicitly revealed by eq. (1). This problem may be eliminated if we use the modified equation suggested by Khanna and Taylor¹⁰:

$$\theta_a = \exp(-kt)^n \tag{2}$$

The kinetic parameters are obtained from eq. (2) by plotting the data according to eq. (3):

$$\ln(-\ln \theta_a) = n \ln k + n \ln t \tag{3}$$

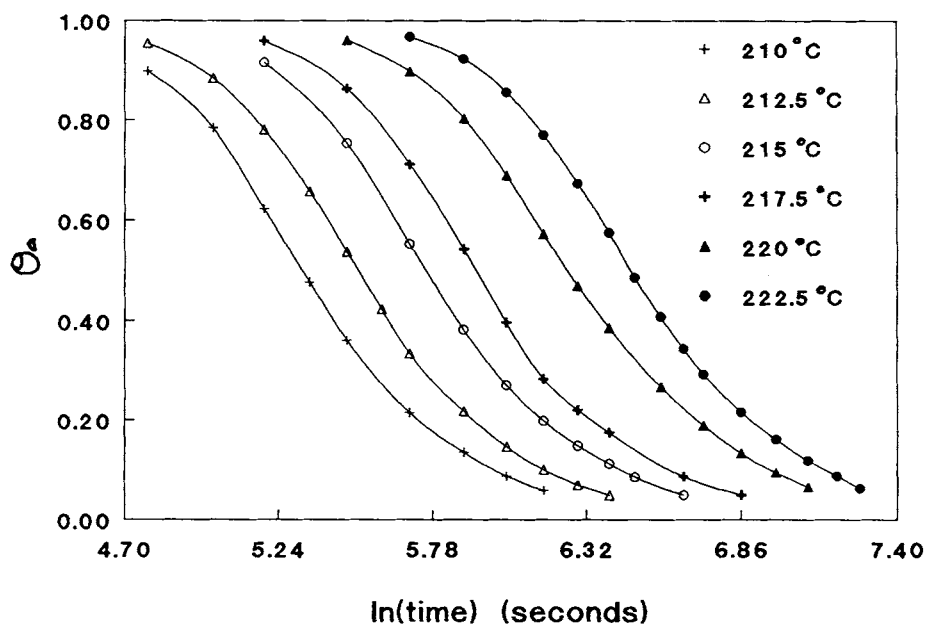


Figure 4 Crystallization isotherms at various temperatures for PET (1.4% DEG); I.V. = 0.71.

Table II Half-Times and Induction Times (in Minutes) for Different PET Samples when Crystallized Isothermally from the Melt

Temp (°C)	1.4% DEG		2.08% DEG		2.94% DEG	
	t_{ind}	$t_{0.5}$	t_{ind}	$t_{0.5}$	t_{ind}	$t_{0.5}$
210.0	0.8	3.4	0.9	3.8	1.2	6.1
212.5	0.9	4.2	1.1	4.5	1.8	8.0
215.0	1.2	5.3	1.4	5.6	2.2	11.0
217.5	1.5	6.3	2.0	8.9	3.2	14.5
220.0	1.8	8.7	2.3	11.9	3.9	18.1
222.5	2.6	10.9	4.0	17.2		

Therefore, a plot of $\ln(-\ln \theta_a)$ vs. $\ln t$ yields a straight line; the slope is equal to n and the intercept is equal to $n \ln k$. Typical Avrami plots for the crystallization behavior of PET with 1.4% DEG at different temperatures are given in Figure 5. Similar data were obtained for the other two samples. The straight line at lower conversions represents primary crystallization and the one at higher conversions represents secondary crystallization. The values of k and n for primary crystallization are listed in Table III. The value of k decreases with increasing DEG content. The values of n are around 3 for all the samples. This indicates either a homogeneous disc-like or a heterogeneous spherulitic structure. Yu et al.¹ studied the morphology of PET samples con-

taining DEG and observed a spherulitic structure. Since the value of n is similar for all the samples, the mechanism of crystallization is not affected by the DEG content.

All PET samples exhibited secondary crystallization when the degree of crystallinity exceeded 75% of the total potential crystallinity. The values of n for secondary crystallization are listed in Table IV. The values are less than those for primary crystallization. This is consistent with the lower values of n for secondary crystallization reported by Yu et al.¹

The results of the present study of isothermal crystallization of PET from the melt confirm the conclusions made in previous publications.^{1,2,4} The rate of crystallization is reduced due to the increased

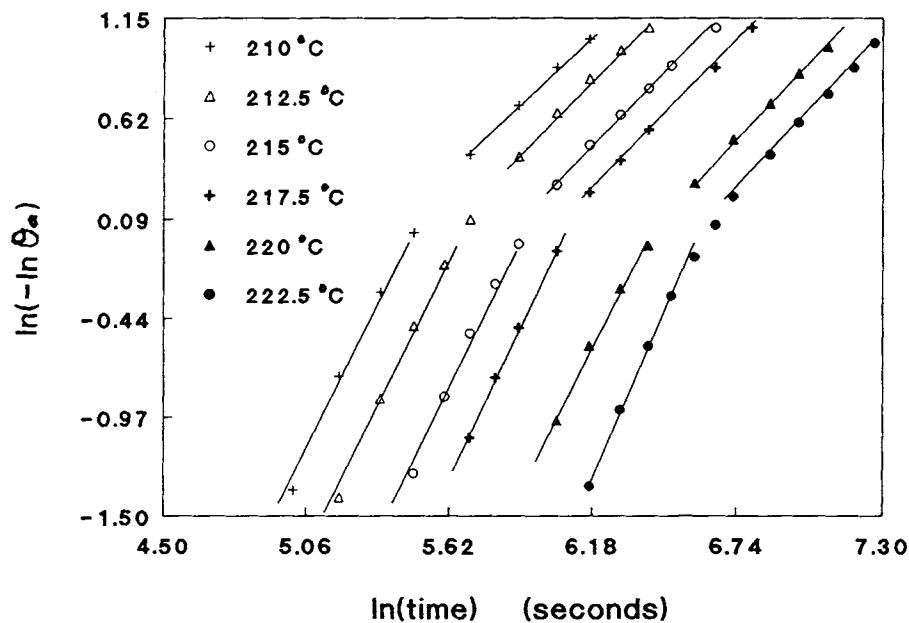


Figure 5 An Avrami plot for isothermal crystallization at various temperatures for PET (1.4% DEG); I.V. = 0.71.

Table III Values of Rate Constant, k , and Avrami Exponent, n , for Different PET Samples when Crystallized Isothermally from the Melt

Temp (°C)	1.4% DEG		2.08% DEG		2.94% DEG	
	n	$k \times 10^3$	n	$k \times 10^3$	n	$k \times 10^3$
210.0	2.9	4.2	3.0	3.8	3.0	2.4
212.5	3.0	3.5	3.0	2.8	3.0	1.8
215.0	3.0	2.8	3.1	2.4	2.9	1.4
217.5	2.9	2.3	3.0	1.8	3.0	1.0
220.0	3.0	1.7	3.1	1.4	3.0	0.8
222.5	3.0	1.4	3.1	1.1		

$$k = \text{s}^{-1}.$$

concentration of DEG. Frank and Zachmann² attributed this to the decrease in the apparent degree of supercooling ($\Delta T = T_m^0 - T_c$), where T_c is the crystallization temperature. Since T_m^0 decreases with increasing DEG content, at the same crystallization temperature, the apparent degree of supercooling is less for samples with higher DEG content. This causes the crystallization rate to decrease. But Figure 6 shows that even for the same ΔT the crystallization rate was lower for samples with higher DEG content. This, as explained by Yu et al.,¹ is due to the irregularities introduced by DEG in the PET structure. For the samples with higher DEG content, there are more irregularities and, hence, the rate is lower. Thus, the decrease in the crystallization rate with increasing DEG content is partly due to the lower degree of supercooling and partly due to the irregular crystal structure caused by DEG.

Isothermal Crystallization from the Glassy State

The results were analyzed in a manner similar to that used for isothermal crystallization from the melt. The half-times of crystallization for various DEG contents are listed in Table V. The half-times for the lowest and the highest DEG content are almost the same but they are lower for 2.08% DEG. The values of k and n as shown in Table VI also show that the rate of crystallization is slightly higher for the sample with 2.08% DEG. A wider range of DEG contents would have to be investigated to fully understand the effect of DEG on the crystallization from the glassy state.

The values of n are in the range 1–2. Jabarin¹¹ also reported lower values of n for crystallization from the glassy state. Thus, the mechanism of crystallization is different when crystallizing from the

glassy state compared to that when crystallizing from the melt.

Yu et al.¹ studied crystallization from the glassy state of PET samples containing up to 15 mol % DEG. They found that DEG has only a weak influence on the crystallization of PET at lower temperatures. The results of the current study are consistent with those of Yu et al.¹ Golike and Cobbs⁴ found that at lower temperatures the rate of crystallization increases with increasing DEG contents. They attributed this to the flexible aliphatic chains introduced by the presence of DEG.

Theory

Crystallization in polymeric materials is generally nucleation-controlled. By means of classical nucleation theory, the energetics of formation of the nuclei are examined. The rate at which the nucleation occurs at constant temperature and pressure is given by^{12,13}

$$N = N_0 \exp(-\Delta E/k_b T_c) \exp(-\Delta G^*/k_b T_c) \quad (4)$$

Table IV Values of Avrami Exponent, n (for Secondary Crystallization), for Different PET Samples when Crystallized Isothermally from the Melt

Temp (°C)	1.4% DEG	2.08% DEG	2.94% DEG
210.0	1.3	1.0	1.4
212.5	1.3	1.3	1.3
215.0	1.3	1.5	1.6
217.5	1.4	1.5	1.8
220.0	1.4	1.7	2.1
222.5	1.4	1.8	

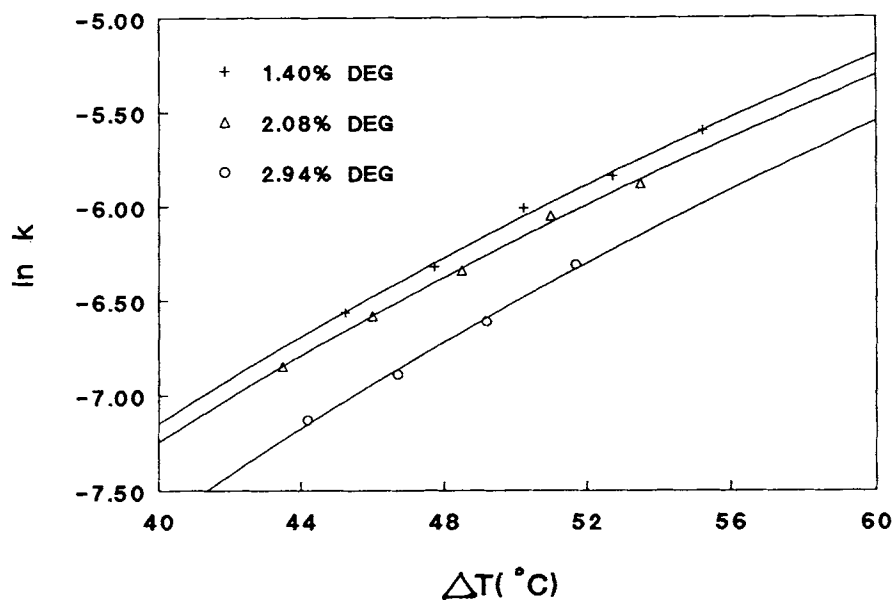


Figure 6 Dependence of crystallization rate on the degree of supercooling.

where N is the nucleation rate; N_0 , a preexponential temperature independent constant, ΔE , the temperature-dependent energy of activation for transport from the isotropic phase; ΔG^* , the critical free energy of the critical-sized nuclei, and k_b and T_c , the Boltzmann constant (1.38×10^{-23} J/K) and the crystallization temperature, respectively.

If the linear crystal growth rate, G , is assumed to be a nucleation-controlled process, then nucleation theory may be utilized to describe the linear growth rate of the crystalline phase as

$$G = G_0 \exp(-\Delta E/k_b T_c) \exp(-\Delta G_g^*/k_b T_c) \quad (5)$$

where ΔG_g^* is the free energy of formation of the secondary nuclei.

In the absence of independent values of N and G , the Avrami temperature-dependent rate parameter, k , may be utilized through the relationship

$$k = NG^z \quad (6)$$

where z is the growth dimensionality of the macroscopic crystallites (and is not equivalent of the Avrami n when the nucleation is homogeneous). From the Avrami kinetics, the value of n was found to be 3. Since the morphology of PET when crystallized from the melt is spherulitic,¹ it is concluded that nucleation is heterogeneous. Hence, the nucleation rate N is a constant and $z = n = 3$. From eqs. (4) and (5), it is possible to generate an equation of the form

$$\ln k = C_0 - z\Delta G_g^*/k_b T_c \quad (7)$$

where C_0 is a constant incorporating the nucleation rate N and G_0 . The transport term, $\Delta E/k_b T_c$, is neglected.

For spherulitic morphology of crystallites, assuming the crystallization to be in Regime II as suggested by Palys and Phillips,¹⁴

$$\Delta G_g^* = 2b_0\sigma\sigma_e T_m^0 / \Delta H \Delta T, \\ \ln k \sim C_0 - 2zb_0\sigma\sigma_e T_m^0 / k_b \Delta H T_c \Delta T \quad (8)$$

where T_m^0 is the equilibrium melting temperature; ΔT , the degree of supercooling ($T_m^0 - T_c$); b_0 , the spacing of the crystal planes parallel to the growth surface; σ and σ_e , the lateral and end surface excess free energies, respectively, and ΔH , the enthalpy of fusion. For PET, the values of ΔH and b_0 as reported by Palys and Phillips¹⁴ are 1.8×10^8 J/m³ and 5.53 Å, respectively.

Information about the surface free energies of the critical nuclei may be obtained from the slope of a

Table V Half-Times (in Minutes) for Different PET Samples when Crystallized Isothermally from the Glassy State

Temp (°C)	1.40% DEG	2.08% DEG	2.94% DEG
115.0	13.0	9.0	12.5
117.5	8.0	5.5	9.3
120.0	5.4	4.1	5.0
125.0	4.6	2.8	4.2

Table VI Values of Rate Constant, k , and Avrami Exponent, n , for Different PET Samples when Crystallized Isothermally from the Glassy State

Temp (°C)	1.4% DEG		2.08% DEG		2.94% DEG	
	n	$k \times 10^3$	n	$k \times 10^3$	n	$k \times 10^3$
112.5	1.8	0.7	1.6	1.3	2.1	0.8
115.0	1.8	1.1	1.5	1.5	1.9	1.1

$k = \text{s}^{-1}$.

plot of $\ln k$ vs. $T_m^0/T_c\Delta T$. This plot is shown in Figure 7 and the values of $\sigma\sigma_e$ are listed in Table VII. The values compare well with those of $1940 \times 10^{-6} \text{ J}^2 \text{ m}^{-4}$ by Palys and Phillips¹⁴ and $80 \times 10^{-6} \text{ J}^2 \text{ m}^{-4}$ reported by Baranov et al.¹⁵ considering the approximation made in eq. (8). The values of $\sigma\sigma_e$ are around 192×10^{-6} for all the samples. They do not change with change in DEG content. A change in morphology of the crystallites causes a change in the value of $\sigma\sigma_e$. Thus, the morphology of the crystallites is not affected by the DEG content.

Dynamic Crystallization

The fraction of the material transformed, $\alpha(T)$ at any temperature T , is calculated by

$$\alpha(T) = \Delta H_T / \Delta H_c$$

where ΔH_T is the heat of crystallization at that temperature and ΔH_c is the heat of crystallization at the end of the cooling process.

The Avrami equation describing the isothermal crystallization has been extended by Ozawa¹⁶ for the nonisothermal kinetic process. The modified Avrami equation is given by

$$1 - \alpha(T) = \exp[-k(T)/R^n] \quad (9)$$

where $\alpha(T)$ is the amount of material transformed at temperature T ; $k(T)$, the rate of crystallization; R , the cooling rate; and n , the Avrami exponent.

The suggested modification of the Avrami equation made by Khanna and Taylor¹⁰ as indicated in eq. (2) is now applied to eq. (9):

$$1 - \alpha(T) = \exp[-k(T)/R]^n \quad (10)$$

$$\ln\{-\ln[1 - \alpha(T)]\} = n \ln k - n \ln R \quad (11)$$

Typical plots of the above equation are shown in Figure 8. The values of k and n are listed in Table VIII.

Thus, in the case of dynamic crystallization from the melt, the rate of PET crystallization also de-

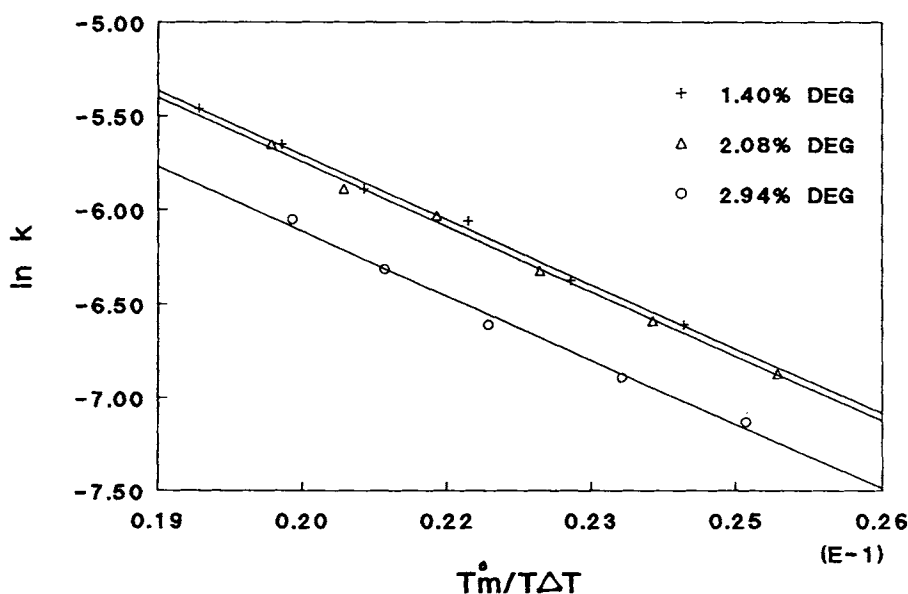


Figure 7 Plot of $\ln k$ vs. $T_m^0/T_c\Delta T$ for PET samples of various DEG contents.

Table VII Values of Lateral and End Surface Free Energies $\sigma\sigma_e$ for Different PET Samples

DEG (wt %)	$\sigma\sigma_e$ (J^2/m^{-4})
1.40	191.6×10^{-6}
2.08	192.2×10^{-6}
2.94	191.4×10^{-6}

creases with increasing DEG content. It should be noted that the value of n is about 1. Thus, when crystallizing dynamically, the mechanism of crystallization is different from that occurring during isothermal crystallization. An analysis of the crystallization of different PET samples done by Jabarin¹⁷ showed that samples provided by Eastman differed in mechanism when crystallized dynamically and isothermally; the others had the same value of n for isothermal and dynamic crystallization, indicating different morphologies between the two methods of crystallization. The analysis of dynamic crystallization is done for degree of crystallization less than 75%. Hence, secondary crystallization that occurs at higher conversions is not seen in Figure 8.

Strain-Induced Crystallization

When a polymer sample is stretched under appropriate conditions, the chains align themselves in the

direction of stretching, causing the sample to crystallize. This is different from the crystallization described earlier where heat induced the sample to crystallize.

PET samples, in the form of sheets, were stretched in the LET at different strain rates at 100°C. The orientation was biaxial and simultaneous, i.e., the samples were stretched in both the x and y directions simultaneously. The variations of the elongational force with the extension ratio at various stretch rates are shown in Figure 9 for the PET sample with 1.40% DEG. The curves obtained for the samples with higher DEG contents are similar in nature. The shapes of the load-extension curves resemble those described earlier by Jabarin.⁶ In general, these curves consist of three regions: The first region is the result of simple elastic elongation and extends to the yield point. In the second region, molecular alignment takes place in the direction of stretch. The force remains constant over this region. In the third region, there is an upward swing in the force that is referred to as the strain-hardening phenomenon. The second region is the one where strain-induced crystallization can be expected to occur. Hence, a stretch ratio of 3×3 was selected for the study of strain-induced crystallization.

PET samples with the highest and lowest DEG contents were stretched 3×3 at different rates (0.25, 0.5, 1 in./s) and annealed for different amounts of times ranging from 0 to 10 min at 100°C. The temperature was chosen such that it was well above T_g .

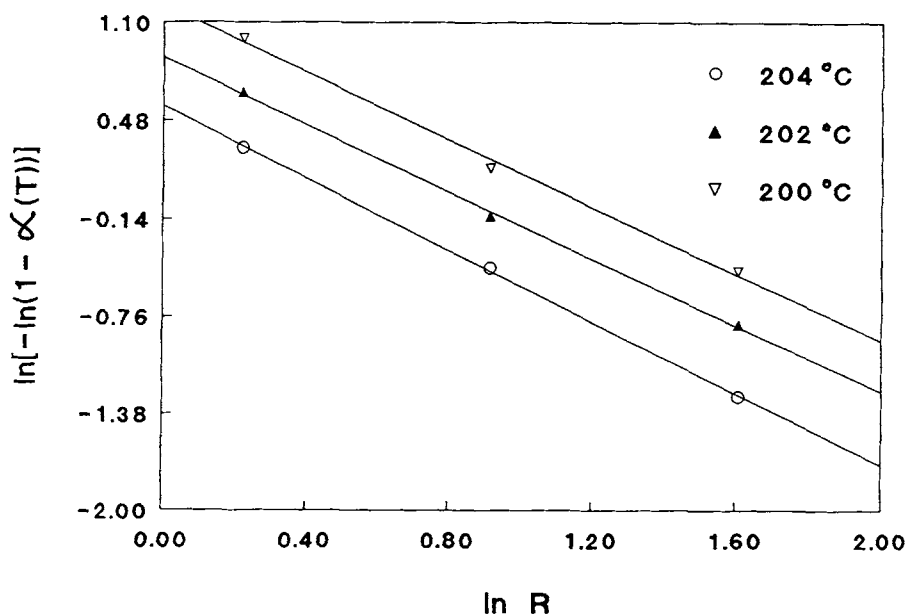


Figure 8 An Avrami plot for dynamic crystallization at various temperatures for PET (1.4% DEG); I.V. = 0.71.

Table VIII Values of Rate Constant, k , and Avrami Exponent, n , for Different PET Samples when Crystallized Dynamically from the Melt

Temp (°C)	1.4% DEG		2.08% DEG		2.94% DEG	
	n	k	n	k	n	k
204	1.1	1.7				
202	1.0	2.3				
200	1.1	3.1	1.1	2.0		
198			1.0	2.8		
196			1.0	3.9	1.3	1.8
194					1.1	2.4
192					1.1	3.1

$k = \text{deg/min.}$

The stretched samples were then evaluated for crystallinity by measuring their density and birefringence values.

The birefringence of an oriented polymer sample is given by¹⁸

$$\Delta = \beta \Delta_{cr} f_{cr} + \beta \Delta_{am} f_{am}$$

where Δ_{cr} and Δ_{am} are the birefringence values of perfectly oriented crystalline and amorphous phases, respectively. The orientation functions of the crystalline and amorphous phase are f_{cr} and f_{am} , respectively. The volume fraction of crystallinity of the sample is β . Thus, Δ is a measure of the crystallinity of the sample.

Figures 10–13 show plots of density and birefringence vs. annealing times of the two samples. At low strain rates (0.25 in./s), as seen in Figures 10 and 11, the density and birefringence increase slowly at the beginning and then at a faster rate before leveling off. At the strain rate of 1 in./s (Figs. 10 and 11), there is a rapid increase in birefringence and density before leveling off. This is because, at high speed, strain-induced crystallization occurs rapidly during the stretching process. Further annealing does not cause the crystallinity to increase further. In both cases, the DEG content has no effect on the crystallization. At the strain rate of 0.5 in./s (Figs. 12 and 13), the sample with the higher DEG content was found to have lower density and birefringence values.

Thus, at low strain rates, when the degree of crystallization is low, and at high strain rates, when the rate of crystallization is very fast, the DEG content has no appreciable effect on the crystallization of PET. At low strain rates, there is little crystallization, and at high strain rates, the rate of stretching is so high that the DEG molecules do not obstruct the orientation process. But at intermediate strain rates, the amount of crystallization decreases with increase in DEG content. This is because at the strain rate of 0.5 in./s the strain rate is not high enough for the PET chains to align themselves without being obstructed by DEG. Because of this, the level of orientation is lower for samples with higher DEG contents.

The three samples were stretched at different strain rates (0.1, 1, 4 in./s) and quenched imme-

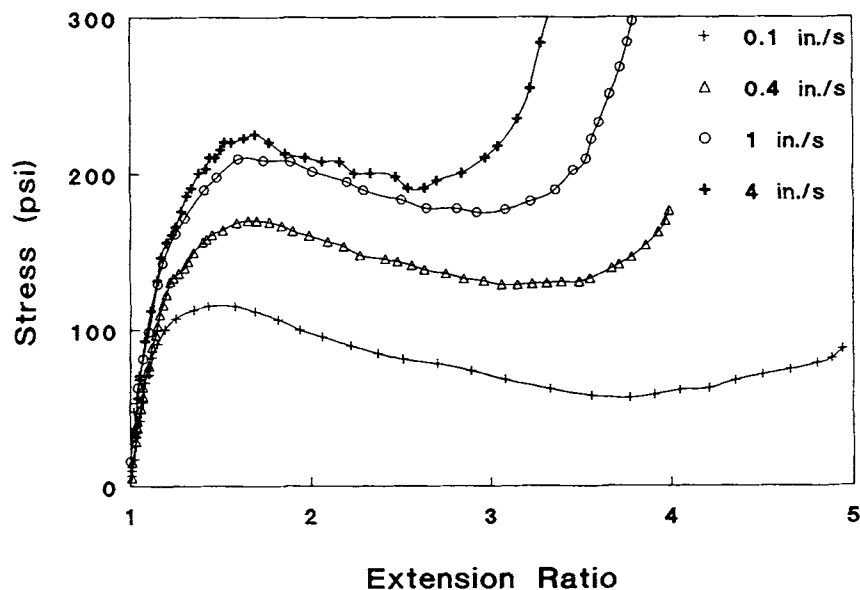


Figure 9 Stress-strain curves for PET (1.4% DEG) at various strain rates.

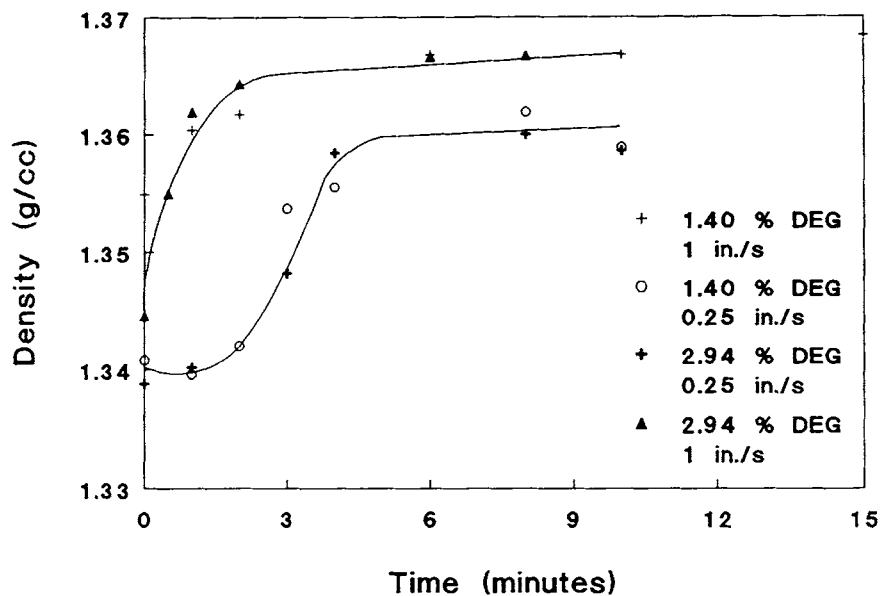


Figure 10 Density as a function of annealing time at strain rates of 0.25 and 1 in./s.

diately. Their density and birefringence values are plotted in Figures 14 and 15, respectively. Both birefringence and density increase with strain rate. At low stretching speed, the rate of relaxation of chains to their random configuration is faster than the rate of chain alignment. At sufficiently high strain rate, the chain alignment overcomes the rate of chain relaxation. Hence, the level of crystallinity at high strain rates is high. It is seen that at high strain rates the level of crystallinity of all the samples is

the same, but at intermediate orientation levels, the sample with the lowest DEG level shows the highest crystallinity, while the other two samples have the same amount of crystallinity.

CONCLUSIONS

The glass transition temperature and the equilibrium melting temperature decrease with increasing

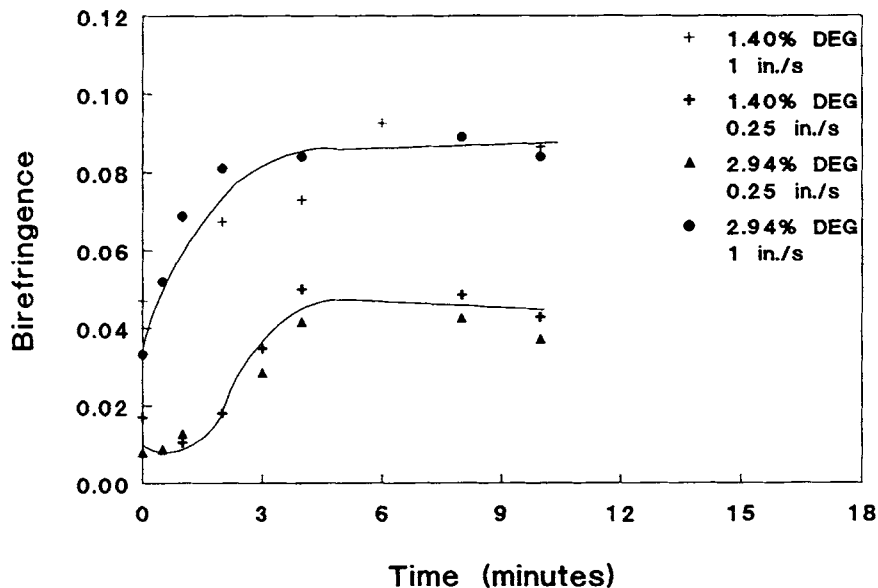


Figure 11 Birefringence as a function of annealing time at strain rates of 0.25 and 1 in./s.

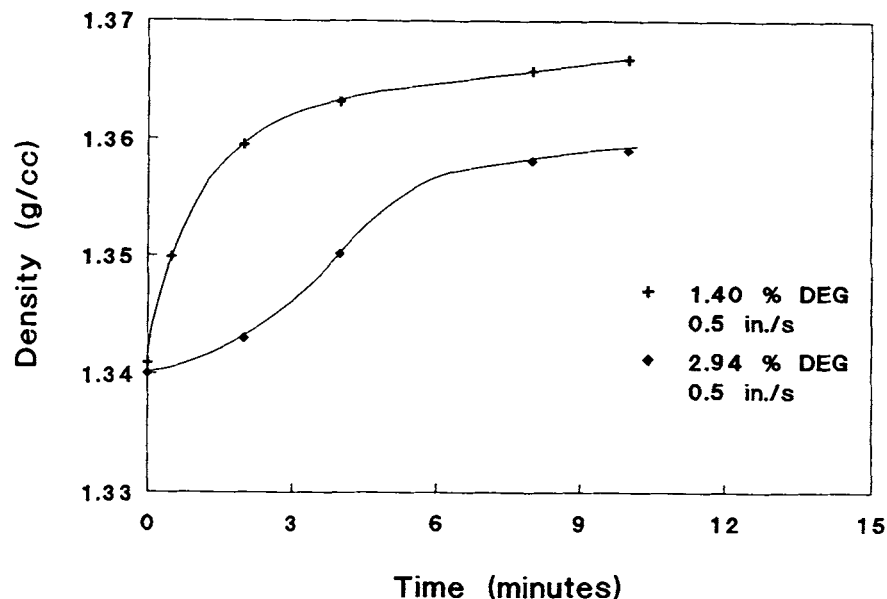


Figure 12 Density as a function of annealing time at a strain rate of 0.5 in./s.

DEG content. As explained by Yu et al.,¹ the decrease in T_g is due to the increase in the ratio of the aliphatic to the aromatic part that results in the increase in flexibility of the main chains. T_m decreases because crystal imperfections arise due to the presence of DEG.

The DEG content reduces the rate of crystallization of PET when crystallizing isothermally from the melt. This is evident from the higher values of half-times and the lower values of rate constant, k ,

as the DEG content increases. The presence of DEG hinders the alignment of PET chains and, hence, reduces the rate of crystallization. The mechanism of crystallization is not affected by the DEG content as the value of the Avrami exponent, n , is the same for all DEG contents. Although the current study did not address the study of the morphology of crystallites, Yu et al.,¹ using light microscopy and light scattering, found the crystallites to have a spherulitic structure. This corresponds to the value of 3 ob-

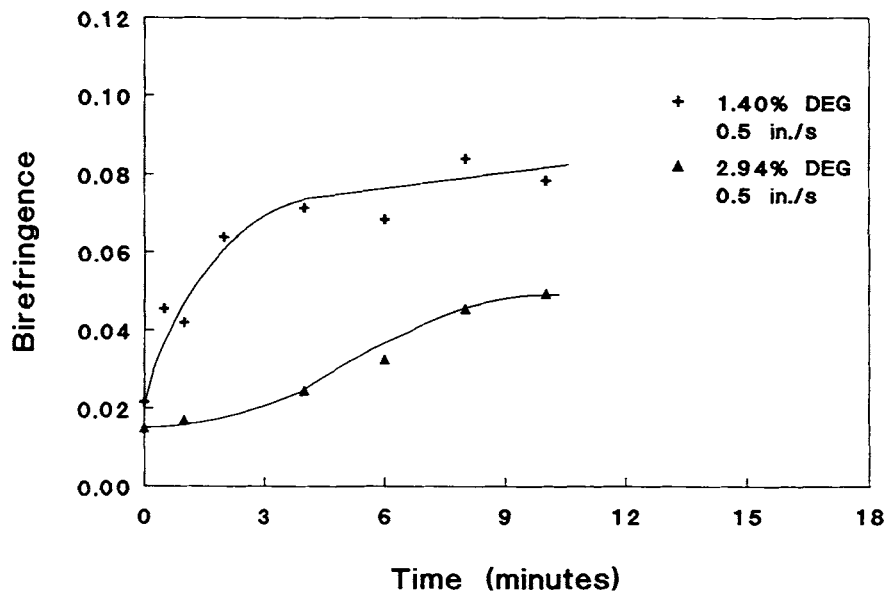


Figure 13 Birefringence as a function of annealing time at a strain rate of 0.5 in./s.

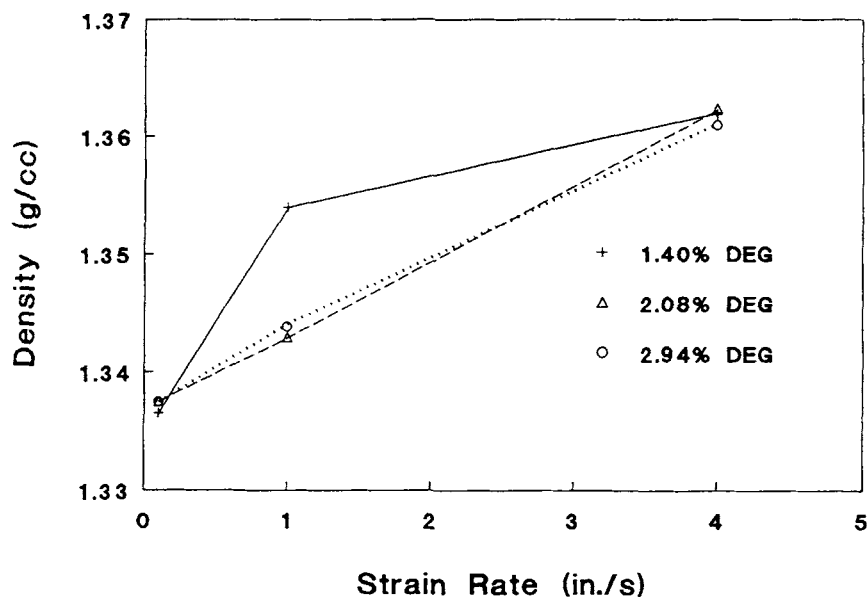


Figure 14 Density as a function of strain rate for different PET samples.

tained for n in our experiments. They also found the morphology of the crystallites to change as the DEG content was increased to above 10%. All samples exhibit secondary crystallization. The value of n for secondary crystallization is less than that for primary crystallization.

When crystallizing isothermally from the glassy state, the effect of DEG is not very prominent within the range of DEG contents studied. A wider range of DEG contents would give a better idea of the effect of DEG.

The values of the surface free energies are almost the same for all the samples. Thus, the morphology of the crystals for the three samples is the same. The values are in good agreement with those reported in previous studies.^{14,15} These values could change for higher DEG contents due to changes in morphology.

The mechanism for dynamic crystallization is different from that for isothermal crystallization as seen from the differences in n . This is typical of Eastman PET. The difference in mechanism could

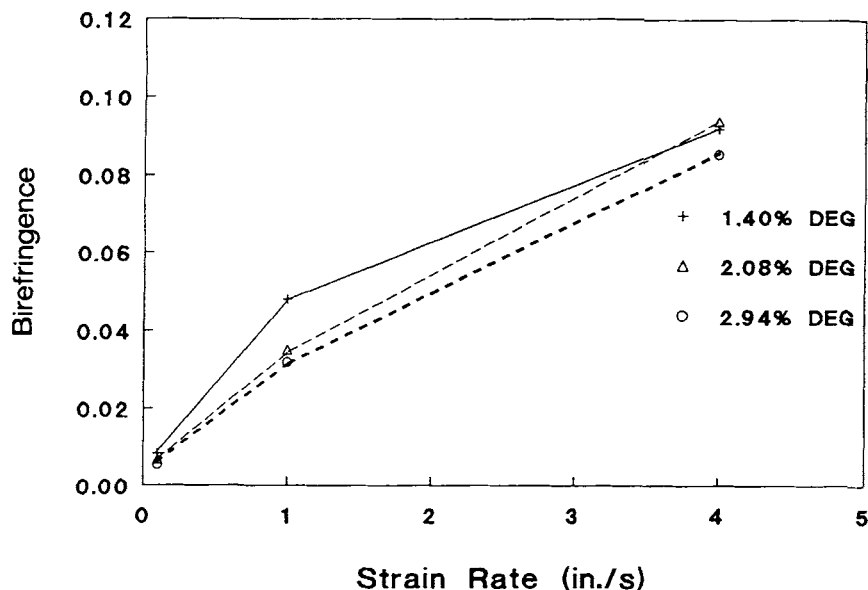


Figure 15 Birefringence as a function of strain rate for different PET samples.

be due to the catalyst system used during the manufacturing process.

All three samples exhibit strain-induced crystallization. At low and high strain rates, the crystallinity is unaffected by the DEG contents. At low strain rates, very low crystallinity is observed. At high rates, the rate of crystallization is fast. At intermediate levels, the sample with the lowest DEG contents shows the highest level of crystallinity.

REFERENCES

1. T. Yu, H. Bu, J. Chen, J. Mei, and J. Hu, *Makromol. Chem.*, **187**, 2697 (1986).
2. W. P. Frank and H. G. Zachmann, *Progr. Colloid Polym. Sci.*, **62**, 88 (1977).
3. S. Farikov, I. Seganov, and J. M. Schultz, *J. Appl. Polym. Sci.*, **32**, 3371 (1986).
4. R. C. Golike and W. H. Cobbs, Jr., *J. Polym. Sci. Polym. Phys. Eds.*, **54**, 277 (1961).
5. S. Farikov, *Polymer*, **21**, 373 (1980).
6. S. A. Jabarin, *Polym. Eng. Sci.*, to appear.
7. S. Okajima, Y. Koizumi, and K. Kagaku, *Zusshi*, **42**, 810 (1939).
8. B. S. Morra and R. S. Stein, *J. Polym. Sci. Polym. Phys. Eds.*, **20**, 2244 (1982).
9. L. Mandelkern, *Crystallization of Polymers*, McGraw Hill, New York, 1964.
10. Y. P. Khanna and T. J. Taylor, *Polym. Eng. Sci.*, **28**, 1042 (1988).
11. S. A. Jabarin, *J. Appl. Polym. Sci.*, **34**, 103 (1987).
12. J. D. Hoffman, G. T. Davis, and J. J. Lauritzen, in *Treatise on Solid State Chemistry*, Vol. III, N. B. Hannay, Ed., Plenum, New York, 1976, Chap. 7.
13. R. J. Ciora and J. H. Magill, *Macromolecules*, **23**, 2350 (1990).
14. L. H. Palys and P. J. Phillips, *J. Polym. Sci. Polym. Phys. Ed.*, **18**, 829 (1980).
15. V. G. Baranov, A. V. Kenarov, and T. I. Volkov, *J. Polym. Sci. Part C*, **30**, 271 (1970).
16. T. Ozawa, *Polymer*, **12**, 150 (1971).
17. S. A. Jabarin, *J. Appl. Polym. Sci.*, **34**, 97 (1987).
18. R. S. Stein, *J. Polym. Sci.*, **24**, 383 (1957).

Received April 16, 1992

Accepted May 13, 1992